ACS OMEGA

http://pubs.acs.org/journal/acsodf

Article

Verification and Temperature-Dependent Rectification by HBQ, the Smallest Unimolecular Donor−Acceptor Rectifier

Yingmei Han, Li Jiang, Joseph E. Meany, Yulong Wang, Stephen A. Woski, Marcus S. Johnson, Christian A. Nijhuis, and Robert M. Metzger*

Cite This: *ACS Omega* 2022, 7, 28790−28796

Read Online

ACCESS | Metrics & More | Article Recommendations | Supporting Information

ABSTRACT: Five years ago, rectification of electrical current was found in 4′-bromo-3,4-dicyano-2′,5′-dimethoxy-[1,1′-biphenyl]-2,5-dione (**1**), a hemibiquinone (which we will call either **1** or HBQ) that has a very small working length (1.1 nm). Monolayers of HBQ on Au^{TS} were detected by "nanodozing" atomic force microscopy (AFM) and were contacted with two types of top electrodes: either cold Au or eutectic Ga−In. Here, we describe cyclic voltammetry of a self-assembled monolayer (SAM) of HBQ and its orientation on a gold substrate with angle-resolved X-ray photoelectron spectroscopy. New measurements of its rectification as a monolayer as a function of bias range and temperature confirm and prove that HBQ is truly the smallest donor−acceptor rectifier and provide some insight into the mechanism of rectification.

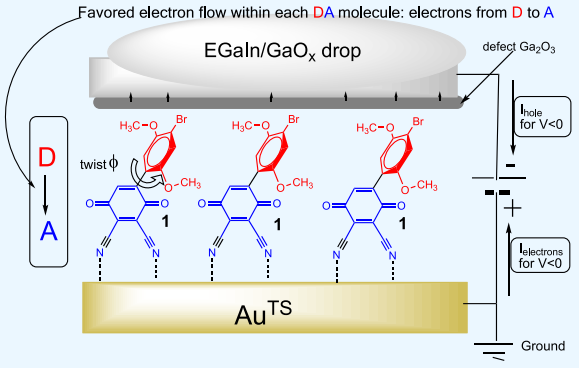

INTRODUCTION

In the last several years, electrical properties of molecular wires and rectifiers have been studied intensively all over the world.[1−22] Over 50 unimolecular rectifiers have been measured either as a single molecule or as a monolayer,[2] but other types have been studied as well.[10−22] Most rectifiers consist of an electron-donating part (D) with a comparatively high-lying highest occupied molecular orbital (HOMO) and an electron-accepting part (A) with a comparatively low lowest unoccupied molecular orbital (LUMO). The working direction of all measured organic rectifiers shows the electron moving more easily from D to A than from A to D. Most rectifiers[2−9] also have a short covalent bridge B, typically saturated and denoted "σ" linking D to A and depicted as D−σ−A. In contrast, HBQ does not have such a bridge.

The D-to-A electronic asymmetry in "metal/molecule/metal" junctions (also called "sandwiches"[2]) is logically akin to the asymmetry present in bulk inorganic pn junction rectifiers. This asymmetry is quantified by the voltage-dependent rectification ratio RR of the current I at a given applied voltage V, as given by eq 1. Equation 1 also defines the direction of rectification where the current is allowed to pass the junction at either positive (+) or negative (−) applied V: in our experiments, the bias (positive or negative) was applied to the top electrode, while the bottom electrode was connected to the ground, i.e., it was held at $V = 0$

$$+\mathrm{RR} = I(V)/I(-V)$$
$$-\mathrm{RR} = I(-V)/I(V) \quad (1)$$

The concept of a unimolecular D−σ−A rectifier was first proposed by Aviram and Ratner.[23] The D−σ−A molecules must be in order so that in a monolayer the D is always, say, "on the left", and "A" is on the right. Langmuir−Blodgett ordering is achieved when one side of the molecule is more hydrophilic than the other.[24] Chemisorptive ordering as a self-assembled monolayer (SAM) is achieved when group(s) that can bond covalently to a metal electrode is(are) found only on one side of the molecule.

For many years, the design "mantra" of an optimal D−σ−A rectifier consisted of three design criteria. First, one should focus on as potent donors D (low ionization potentials) as possible and as powerful acceptors A (high electron affinities) as possible. Second, the electronic properties of the D and A components are usually preserved in the D−σ−A molecule by linking the D-to-A moieties with a saturated "sigma bridge σ" of 3−6 C atoms.[2] One should think about an "actual" rectifying molecule as σ_D−D−σ−A−σ_A, where, in addition to the bridge σ, one or two other linkage/assembly tails σ_D and/or σ_A allow physisorptive (Langmuir−Blodgett) or chemisorptive (self-assembled monolayer) ordering on a substrate or between substrates. Third, if one wants a precise and

Received: March 10, 2022
Accepted: June 30, 2022
Published: August 10, 2022

Scheme 1. Chemical Structure of Three 4′-Bromo-3,4-dicyano-2′,5′-dimethoxy-[1,1′-biphenyl]-2,5-dione (HBQ) Molecules 1 (to Signify a Monolayer), Embedded in an Au^{TS}-HBQ//GaO_x/EGaIn Sandwich and Connected to the External DC Voltage Shown When HBQ Rectifies (Electron Flow from D to A) at $V = -2.5$ V[a]

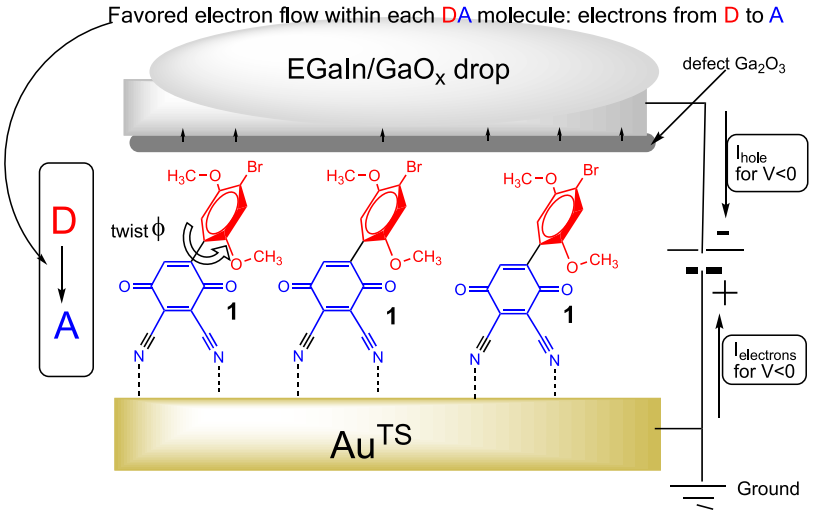

[a]The diagram also shows the very important twist angle ϕ between D and A, that insulates the orbitals mostly localized on D from those mostly localized on A.

distinctive rectifying electron flow, then bridge σ, σ_D, and/or σ_A should be as short as possible.

The recent rectifier HBQ **1** does not adhere to two of the three design criteria enunciated: (1) D = (1,4-dimethoxyhydroquinone) is a weak donor, not a strong donor, while A = (2,3-dicyano-1,4-benzoquinone) is only a moderate acceptor. (2) Instead of a σ bridge, the large intramolecular twist angle ϕ prevents steric crowding in HBQ and isolates the HOMO (mostly localized on the D moiety) from the LUMO (mostly localized on the A moiety).[1] (3) Criterion three survives: the tail(s) are two cyano groups of minimal length that chemisorb on Au. The experimental situation is shown in Scheme 1.

A technologically important issue has been that the measured RR for unimolecular devices has, in general, remained small (RR = 20−3000), compared with inorganic pn junction rectifiers that have RR in millions.[2−4] This gap has been closed when RR = 6.3×10^5 was found recently for an alkylferrocenyl-ethynyl-ferrocene monolayer sandwiched asymmetrically between a Pt electrode and an EGaIn electrode.[5] This diode, however, stands quite tall, with a length of about 3 nm.

The present contribution complements and deepens earlier work;[1] here, the monolayer of HBQ was studied further by cyclic voltammetry (CV) on Au, by ultraviolet photoelectron spectroscopy (UPS), NEXAFS, etc. The rectification ratio was previously measured in three different types of sandwiches: (i) "EGaIn|Au drop|HBQ monolayer|Au", (ii) "EGaIn|cold Au|HBQ monolayer|Au", and (iii) "Pt−Ir tip|HBQ molecule|Au".[1] Here, we report on HBQ measured (iv) as an "EGaIn|HBQ monolayer|Au" sandwich with greatly improved statistics.

RESULTS AND DISCUSSION

The HBQ molecules were self-assembled on template-stripped Au^{TS} surfaces (Section S1) according to previously reported procedures.[5,25−28] The SAM was characterized by cyclic voltammetry (CV)[1] (Section S2), ultraviolet photoelectron spectroscopy (UPS), and near-edge X-ray adsorption fine structure (NEXAFS) (Section S3) to obtain the electronic and supramolecular structure of the SAM. To obtain more insight about the HOMO and LUMO for the HBQ molecule, we also performed DFT calculations (Section S4) and made further UV−vis measurements (Section S5). Note that X-ray photoelectron spectroscopy data have been reported before.[1]

Scanning Tunneling Microscopy (STM). New but preliminary molecular-scale STM results for a monolayer of HBQ on Au were obtained at Texas A&M University, as shown in Section S7, albeit with the caveat that one student found excellent results, while a second student could not reproduce them.

Cyclic Voltammetry (CV). CV was performed to measure the redox properties of the HBQ SAM (Section S2). The HBQ molecule can be oxidized (to form a radical cation) or reduced (to form a radical anion).[1] Previously reported CV data of HBQ in solution reveal (Figure S1) three pairs of well-resolved redox peaks involving two reduction steps (2/2′ and 3/3′) and one oxidation step (1/1′).[1] The high formal potential ($E_{1/2}$ = 1.197 V vs SCE) of 1/1′ (Table S1) confirms the weak electron−donor property of HBQ.[1]

The cyclic voltammogram of the HBQ SAM on Au^{TS} (Figure 1a) shows that the $E_{1/2}$ of 1/1′ shifts by −420 mV relative to that of the free molecule in solution (Table S1); this shift indicates that HBQ interacts strongly with the surface. Figure 1a shows one reduction step around 0 V (2/2′). Due to the small applied bias window, the second reduction peak was not observed. Figure 1a−c shows scan-rate-dependent CV data and demonstrate the linear relationship between the scan rates and the anodic peak current of 1/1′ and 2/2′ ($i_{a,1}$ and $i_{a,2}$): this confirms that the HBQ molecules are covalently confined to the Au^{TS} surface. The energy of HOMO level (E_{HOMO}) was estimated from CV using a previously reported method (Section S2). Table S2 shows that the determined E_{HOMO} (−5.22 eV) well matches the value obtained from UPS spectra (−5.48 eV).

Photoelectron Spectroscopy Measurements. We performed ultraviolet photoelectron spectroscopy (UPS) to determine the secondary electron cut-off (Figure 1d) and

https://doi.org/10.1021/acsomega.2c01182
ACS Omega 2022, 7, 28790−28796

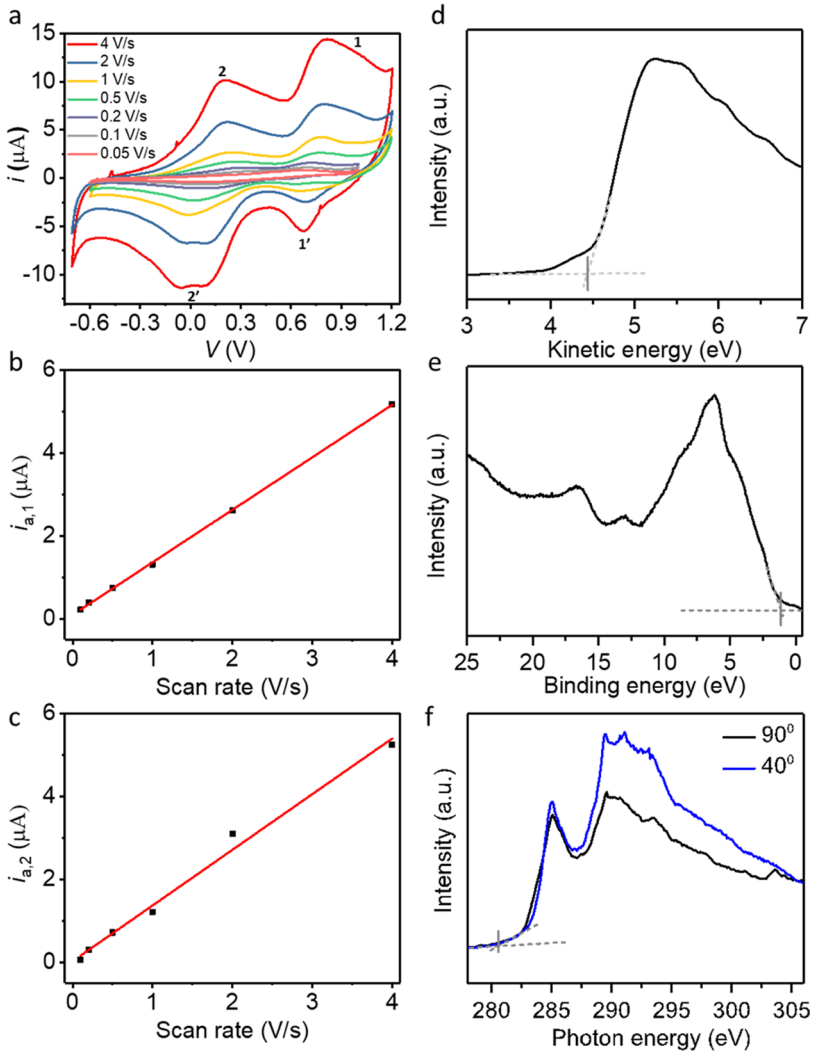

Figure 1. (a) Cyclic voltammogram of HBQ monolayer on Au^{TS} at different scan rates. 1/1′and 2/2′ are the corresponding redox peaks. (b, c) Anodic peak currents (i_{a1} and i_{a2}) vs scan rates for peaks 1 and 2. (d) Secondary electron cut-off (SECO) spectrum of HBQ SAM on Au^{TS}. (e) Valence-band spectrum of HBQ SAM on Au. (f) NEXAFS spectrum of HBQ SAM on Au^{TS} at incident angles of 90° (NI) and 40° (GI).

valence-band spectra (Figure 1e) of the HBQ SAM on Au^{TS}. These measurements allow us to experimentally determine the work function, WF (in eV), and the energy-level alignment of the molecule−electrode interface. More specifically, the energy offset, δE_{HOMO} (in eV), between the energy of highest occupied molecular orbital (HOMO), E_{HOMO} (in eV), and the electrode Fermi level, E_f (in eV), can be determined from the valence-band spectra. This information will help us to elucidate the mechanism of charge transfer as discussed in more detail below. The value of WF after SAM formation is 4.33 eV (Figure 1d and Table S2). This significant reduction of the work function of bare Au^{TS} (5.1 eV) is typical for adsorbates and indicates that push-back effects and surface dipole formation are important after SAM formation,[29] and again confirms that the HBQ molecules interact strongly with Au^{TS}. The value of δE_{HOMO} determined from the valence-band spectra is 1.15 eV (Table S2), leading to the E_{HOMO} value obtained from UPS as −5.48 eV.

To confirm that the molecules form a standing-up phase, we determined the tilt angle with respect to the surface or with near-edge X-ray absorption fine structure (NEXAFS) spectroscopy. The NEXAFS spectra were recorded at incident angles of 90 and 40° and are shown in Figure 1f. The first resonance peak at 285.1 eV is attributed to a σ-to-π^* transition in C═C that we used to determine the tilt angle ϕ by estimating the ratio of the first resonance peak intensity at 40 and 90° (Section S3). The estimated tilt angle was ϕ = 42.5° (Table S2), which confirms the "standing-up" phase of the HBQ SAM.

Density Functional Theory (DFT). The DFT calculation (Section S4) shows that LUMO is mainly located at the benzoquinone part (A), which will delocalize into the Au^{TS} surface when HBQ is self-assembled on the Au^{TS} bottom electrode: this complicates locating the LUMO by a surface characterization method. Therefore, to determine the E_{LUMO}, we recorded the UV−vis spectrum (Section S5) of HBQ in MeCN to obtain the HOMO−LUMO gap (E_{HL}). As shown in Table S2, the obtained E_{HL} = 1.78 eV is consistent with that calculated from DFT (1.59 eV), while from E_{HOMO} (UPS) and E_{HL}, one obtains E_{LUMO} = 3.70 eV.

DFT calculations found an optimal ϕ = 39.7[1] or 38.5°,[3] while the crystal structure of a related dibrominated compound BrHDQBr found a much greater ϕ = 69.1°.[3] Of course, ϕ = 90° would mean complete orthogonalization between orbitals

https://doi.org/10.1021/acsomega.2c01182
ACS Omega 2022, 7, 28790−28796

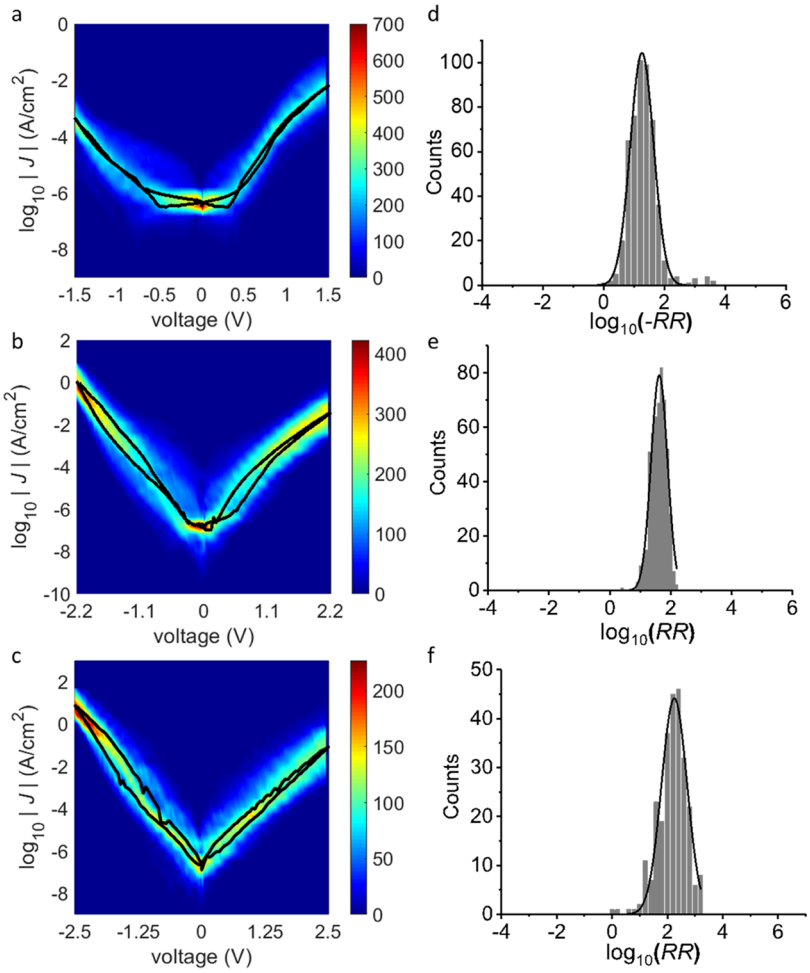

Figure 2. Heat maps of $\log_{10}|J|$ vs V for "Au^{TS}-HBQ|GaO$_x$ |EGaIn" sandwiches with applied bias windows of (a) ±1.5 V, (b) ±2.2 V, and (c) ±2.5 V. Black solid lines are the Gaussian log-averages. Histogram of $\log_{10}$ RR at (d) ±1.5 V, (e), ±2.2 V, and (f) ±2.5 V for "Au-HBQ | GaO$_x$ | EGaIn" sandwiches.

localized on D and orbitals localized on A. Regrettably, no DFT data were reported as a function of how ϕ varies over a large range.

Electrical Measurements. The electrical characterization of self-assembled monolayers (SAMs) of **1** on Au^{TS} bottom electrode was previously performed using three different top electrodes: EGaIn electrode with applied bias window of ±2.5 V,[1] cold top Au electrode with an applied bias window of ±2.5 V,[1] and STM tip with the applied bias window of ±1.5 V.[1] The results showed that the junction can rectify (moderately) at +1.5 V with RR = −6 and rectify even better at −2.5 V with maximum RR = 200. To gain more insights about the electrical characteristics and mechanism of the rectification, we conducted statistical and temperature-dependent electrical measurements of the "Au^{TS}-HBQ/GaO$_x$/EGaIn" sandwich.

The statistically large number of $J(V)$ measurements of the Au^{TS}-HBQ/GaO$_x$/EGaIn sandwiches were conducted using a previously reported method.[5] Figure 2a,d shows the results for an applied bias window of ±1.5 V. The sandwiches rectify at positive bias with RR = −18 (Table S3). With applied bias windows of ±2.2 V (Figure 2b,e) and ±2.5 V (Figure 2c,f), the direction of rectification reverses to RR = 42 (Table S3) and RR = 178 (Table S3), respectively. These results correspond well with those reported previously,[1] but here, we add explanations based on the spectroscopic results described earlier.

Previous work[1] on (i) "EGaIn|Au drop|HBQ monolayer|Au" and (ii) "EGaIn|cold Au|HBQ monolayer|Au" studied in the bias range ±2.5 V[1] did find and report the larger rectification at −2.5 V found here but showed no trace of the smaller rectification at ±1.5 V reported here. The STM data for few molecules of **1** chemisorbed on Au^{TS} did find a smaller rectification at ±1.5 V.[1]

In Figure 2a (scan range ±1.5 V), there is a region of not much current ("Coulomb blockade") within the restricted bias range of ±0.5 V; this Coulomb blockade disappears when the scan range is extended to ±2.5 V (Figure 2c).

We should remember that beyond a bias of ±1 V and in the presence of adventitious H_2O, the "EGaIn" Ga−In eutectic electrode may become electrochemically active, create more Ga^{2+} ions at the interface, and becloud the electrical measurements:[1,30,31] in ref 1, the messier RR of Figure 5B (EGaIn touching the HBQ monolayer) is compared with the simpler RR of Figure 6B (cold Au touching HBQ).

Why do we see a relatively low current between −0.5 and +0.5 V when the scan range is V = ±1.5 V (Figure 2a), which is barely visible in the range V = ±2.2 V (Figure 2b), and is not seen at all when the range becomes V = ±2.5 V? Such behavior is usually labeled Coulomb blockade and attributed to

https://doi.org/10.1021/acsomega.2c01182
ACS Omega 2022, 7, 28790−28796

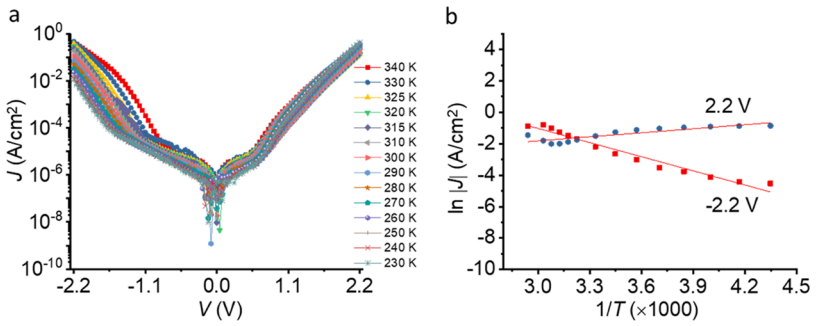

Figure 3. (a) $J(V,T)$ curves for the Au^{TS}-HBQ//GaO$_x$/EGaIn sandwich measured from 340 to 230 K in the bias range ±2.2 V. (b) Arrhenius plots for $J(V,T)$ curves at +2.2 and −2.2 V.

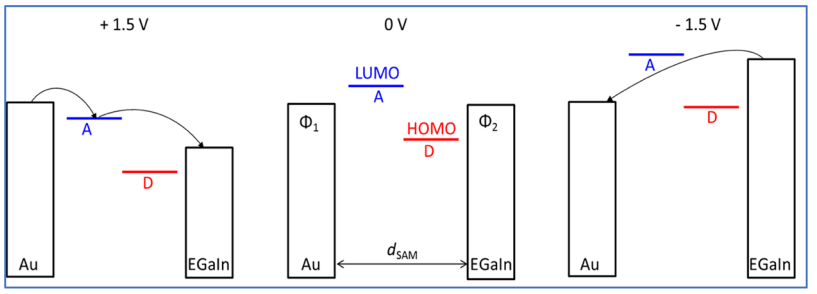

Figure 4. Energy-level diagram of Au^{TS}-HBQ|GaO$_x$|EGaIn sandwich at 0, +1.5, and −1.5 V. Φ_1 and Φ_2 are the work functions of Au and EGaIn, respectively. A denotes the acceptor and D denotes the donor. As already shown in Scheme 1, the template-stripped Au^{TS} is always grounded, at V = 0. The arrows denote the direction of electron transfer. d_{SAM} is the HBQ SAM thickness.

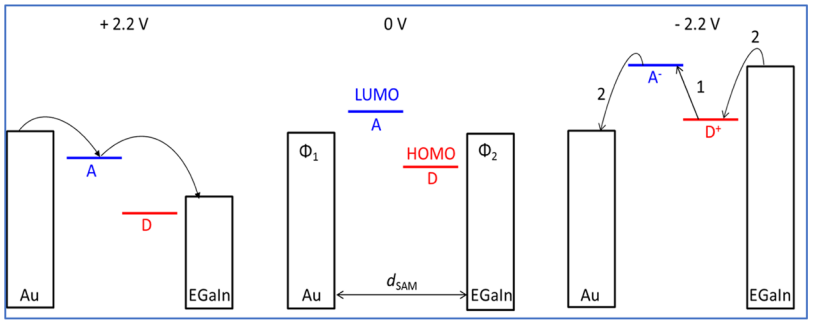

Figure 5. Energy-level diagram of the "Au^{TS}-HBikaelQ|GaO$_x$|EGaIn" sandwich at 0, +2.2, and −2.2 V. Φ_1 and Φ_2 are the work functions of Au and EGaIn, respectively. A stands for acceptor and D stands for donor. As already shown in Scheme 1, the template-stripped Au^{TS} is always grounded, at V = 0. The arrows denote the direction of electron transfer. d_{SAM} is the HBQ SAM thickness.

polarizing either the molecule or the Ga^{+3}O^{-2} couple, always in opposition to the applied bias: this polarization is usually overcome at higher bias.

Coulomb blockades in rectifiers have been seen before[32] and attributed to induced polarization of the monolayer. Remember that a 1.0 V bias across a monolayer of thickness 1.0 nm corresponds to a huge electric field (10^9 V/m). If the Ga layer oxidizes even partially, then the ions and gegenions produced may rearrange in new ways that have escaped facile measurement.

The hysteresis loops seen in Figure 2a and more distinctly in Figure 2b could be due to changes in the twist angle ϕ mentioned in Scheme 1.

Temperature-Dependent J(V) Measurements. For the first rectifier measured by some of us, no temperature dependence of the rectification was found between 370 and 105 K.[33]

To further clarify the mechanism of charge transport across the "Au^{TS}-HBQ//GaO$_x$/EGaIn" sandwich, we performed temperature-dependent $J(V,T)$ measurements using in previously reported procedures[34] (Section S5). Figure 3 shows the $J(V,T)$ measurements with an applied window of ±2.2 V and the corresponding Arrhenius plots. Figure 3b shows that at positive bias, the charge transport shows no activation energy, which is characteristic of coherent tunneling.[35−39] In contrast, at negative bias, the charge transport is thermally activated, with a small activation energy E_a of 250 meV that is characteristic of hopping. Therefore, we conclude that hopping dominates the mechanism of charge transport at negative bias. Note, especially at high T, the RR values are low because hopping dominates at these temperatures.

Energy-Level Diagram. Using the E_{HOMO}, E_{HL}, E_{LUMO}, and WF values obtained from CV, UV−vis, and UPS, we constructed the energy-level diagrams depicted in Figures 4 and 5.

Figure 4 shows that at +1.5 V, the LUMO can participate in the charge transport, resulting in sequential tunneling. In contrast, at −1.5 V, no molecular orbitals can participate in the charge transport, resulting in coherent tunneling. The

https://doi.org/10.1021/acsomega.2c01182
ACS Omega 2022, 7, 28790−28796

sandwich rectifies at +1.5 V. However, when the applied bias is further increased, a large electric field can result as a zwitterion D^+A^- forms, with electron transfer from donor (D) to acceptor (A) (Figure 5). We note that the formation of the zwitterion D^+A^- state has been proposed for other D−A molecules in junctions.[22]

Figure 5 shows that at −2.2 V, after the zwitterion is formed, the second step is two-electron transfers with hopping (from EGaIn to HOMO and from LUMO to Au^{TS}). In contrast, at +2.2 V, only the LUMO can participate in the charge transfer.

Therefore, the electron transport is more efficient at −2.2 V than at +2.2 V, resulting in rectification at −2.2 V.

CONCLUSIONS

The results of ref 1 have been broadly confirmed: HBQ is indeed small and is the first minimal-sized D−A molecule with a commendably large rectification ratio. It is shown by stable EGaIn methods that the rectification ratio for HBQ, quoted previously as between 35 and 180,[1] may actually reach 10^4 after repeated scanning and remarkable stability, which probably is caused by thickening of the gallium-oxide layer.[30] EGaIn electrodes should be used with critical caution for monolayers at biases exceeding ±1 V.

ASSOCIATED CONTENT

Supporting Information

The Supporting Information is available free of charge at https://pubs.acs.org/doi/10.1021/acsomega.2c01182.

Details about self-assembled monolayers; cyclic voltammetry; photoelectron spectroscopy; density functional theory; ultraviolet−visible spectra; statistics on electrical measurements, their stability; and temperature dependence and scanning tunneling spectra (PDF)

AUTHOR INFORMATION

Corresponding Author

Robert M. Metzger − *Department of Chemistry and Biochemistry, University of Alabama, Tuscaloosa, Alabama 35487-0336, United States;* orcid.org/0000-0002-1833-5461; Email: rmetzger@ua.edu

Authors

Yingmei Han − *Department of Chemistry, and Centre for Advanced 2D Materials, National University of Singapore, Singapore 117543, Singapore*

Li Jiang − *Department of Chemistry, and Centre for Advanced 2D Materials, National University of Singapore, Singapore 117543, Singapore*

Joseph E. Meany − *Department of Chemistry and Biochemistry, University of Alabama, Tuscaloosa, Alabama 35487-0336, United States; Savannah River National Laboratory, Aiken, South Carolina 29808, United States*

Yulong Wang − *Department of Chemistry, and Centre for Advanced 2D Materials, National University of Singapore, Singapore 117543, Singapore;* orcid.org/0000-0001-9441-0497

Stephen A. Woski − *Department of Chemistry and Biochemistry, University of Alabama, Tuscaloosa, Alabama 35487-0336, United States*

Marcus S. Johnson − *Department of Chemistry and Biochemistry, University of Alabama, Tuscaloosa, Alabama 35487-0336, United States;* Present Address: SPEX CertiPrep, Methuchen, New Jersey 08840, United States

Christian A. Nijhuis − *Department of Chemistry, and Centre for Advanced 2D Materials, National University of Singapore, Singapore 117543, Singapore; Hybrid Materials for Opto-Electronics Group, Department of Molecules and Materials, MESA+ Institute for Nanotechnology and Center for Brain-Inspired Nano Systems, Faculty of Science and Technology, University of Twente, 7500 AE Enschede, The Netherlands;* orcid.org/0000-0003-3435-4600

Complete contact information is available at: https://pubs.acs.org/10.1021/acsomega.2c01182

Notes

The authors declare no competing financial interest.

ACKNOWLEDGMENTS

The authors acknowledge the National Research Program (award NRF-CRP 8-2011-07) of the Research Foundation of Singapore for supporting this research under the Competitive Research Program. This research was also supported by the NRF, the Prime Minister's Office, Singapore, under its medium-sized Centre Program.

REFERENCES

(1) Meany, J. E.; M S Johnson, M. S.; Woski, S. A.; Metzger, R. M. Surprisingly Big Rectification Ratios for a Very Small Unimolecular Rectifier. *ChemPlusChem* **2016**, *81*, 1152−1155.

(2) Metzger, R. M. Unimolecular Electronics. *Chem. Rev.* **2015**, *115*, 5056−5115.

(3) Meany, J. E.; Kelley, S. P.; Metzger, R. M.; Rogers, R. D.; Woski, S. A. Crystal Structure of 4,4′-Dibromo-2′,5′-dimethoxy-[1,1′-biphenyl]-2,5-dione (BrHBQBr). *Acta Crystallogr., Sect. E: Crystallogr. Commun.* **2015**, *E71*, 1454−1456.

(4) Metzger, R. M. Quo Vadis, Unimolecular Electronics? *Nanoscale* **2018**, *10*, 10316−10332.

(5) Chen, X.; Roemer, M.; Yuan, L.; Du, W.; Thompson, D.; del Barco, E.; Nijhuis, C. A. Molecular Diodes with Rectification Ratios Exceeding 10^5 Driven by Electrostatic Interactions. *Nat. Nanotechnol.* **2017**, *12*, 797−803.

(6) Nichols, R. J.; Higgins, S. J. Single-Molecule Electronics: Chemical and Analytical Perspectives. *Annu. Rev. Anal. Chem.* **2015**, *8*, 389−417.

(7) Sun, L.; Diaz-Fernandez, Y. A.; Gschneidtner, T. A.; Westerlund, F.; Lara-Avila, S.; Moth-Poulsen, K. Single-Molecule Electronics: from Chemical Design to Functional Devices. *Chem. Soc. Rev.* **2014**, *43*, 7378−7411.

(8) Xiang, D.; Wang, X.; Jia, C.; Lee, T.; Guo, X. Molecular-Scale Electronics: From Concept to Function. *Chem. Rev.* **2016**, *116*, 4318−4440.

(9) Su, T. A.; Neupane, M.; Steigerwald, M. L.; Venkataraman, L.; Nuckolls, C. Chemical Principles of Single-Molecule Electronics. *Nat. Rev. Mater.* **2016**, *1*, No. 16002.

(10) Liu, R.; Ke, S.-H.; Yang, W.; Baranger, H. U. Organometallic Molecular Rectification. *J. Chem. Phys.* **2006**, *124*, No. 024718.

(11) Müller-Meskamp, L.; Karthäuser, S.; Zandvliet, H. J. W.; Homberger, M.; Simon, U.; Waser, R. Field-Emission Resonances at Tip/α,ω-Mercaptoalkyl Ferrocene/Au Interfaces Studied by STM. *Small* **2009**, *5*, 496−502.

(12) Yee, S. K.; Sun, J.; Darancet, P.; Tilley, T. D.; Majumdar, A.; Neaton, J. B.; Segalman, R. A. Inverse Rectification in Donor-Acceptor Molecular Heterojunctions. *ACS Nano* **2011**, *5*, 9256−9263.

(13) Hihath, J.; Bruot, C.; Nakamura, H.; Asai, Y.; Díez-Pérez, I.; Lee, Y.; Yu, L.; Tao, N. Inelastic Transport and Low-Bias Rectification in a Single-Molecule Diode. *ACS Nano* **2011**, *5*, 8331−8339.

(14) Mentovich, E. D.; Rosenberg-Shraga, N.; Kalifa, I.; Gozin, M.; Mujica, V.; Hansen, T.; Richter, S. Gated-Controlled Rectification of a Self-Assembled Monolayer-Based Transistor. *J. Phys. Chem. C* **2013**, *117*, 8468−8474.
(15) Arielly, R.; Vadai, M.; Kardash, D.; Noy, G.; Selzer, Y. Real-Time Detection of Redox Events in Molecular Junctions. *J. Am. Chem. Soc.* **2014**, *136*, 2674−2680.
(16) Cui, B.; Xu, Y.; G; Wang, H.; Zhao, W.; Zhai, Y.; Li, D.; Liu, D. A Single- Molecule Diode with Significant Rectification and Negative Differential Resistance Behavior. *Org. Electron.* **2014**, *15*, 484−490.
(17) Trasobares, J.; Vuillaume, D.; Théron, D.; Clément, N. A 17 GHz Molecular Rectifier. *Nat. Commun.* **2016**, *7*, No. 12850.
(18) Jeong, H.; Jang, Y.; Kim, D.; Hwang, W.-T.; Kim, J.-W.; Lee, T. An In-Depth Study of Redox-Induced Conformational Changes in Charge Transport Characteristics of a Ferrocene-Alkanethiolate Molecular Electronic Junction: Temperature-Dependent Transition Voltage Spectroscopy Analysis. *J. Phys. Chem. C* **2016**, *120*, 3564−3572.
(19) Perrin, M. L.; Galán, E.; Eelkema, R.; Thijssen, J. M.; Grozema, F.; van der Zant, H. S. J. A Gate-Tunable Single-Molecule Diode. *Nanoscale* **2016**, *8*, 8919−8923.
(20) Seo, S.; Hwang, E.; Cho, Y.; Lee, J.; Lee, H. Functional Molecular Junctions Derived from Double Self-Assembled Monolayers. *Angew. Chem., Int. Ed.* **2017**, *56*, 12122.
(21) Duche, D.; Planchoke, U.; Dang, F.-X.; Le Rouzo, J.; Bescond, M.; Simon, J.-J.; Balaban, T. S.; Escoubas, L. Model of Self-Assembled Monolayer Based Molecular Diodes Made of Ferrocenyl-Alkanethiols. *J. Appl. Phys.* **2017**, *121*, No. 115503.
(22) Wang, S.; Wei, M.-Z.; Hu, G.-C.; Wang, C.-K.; Zhang, G.-P. Mechanisms of the Odd-Even Effect and Its Reversal in Rectifying Performance of Ferrocenyl-*N*-Alkanethiolate Molecular Diodes. *Org. Electron.* **2017**, *49*, 76−84.
(23) Aviram, A.; Ratner, M. A. Molecular Rectifiers. *Chem. Phys. Lett.* **1974**, *29*, 277−283.
(24) Ashwell, G. J.; Sambles, J. R.; Martin, A. S.; Parker, W. G.; Szablewski, M. Rectifying Characteristics of Mg | ($C_{16}H_{33}$-Q3CNQ LB Film) | Pt Structures. *J. Chem. Soc., Chem. Commun.* **1990**, 1374−1376.
(25) Alloway, D. M.; Hofmann, M.; Smith, D. L.; Gruhn, N. E.; Graham, A. L.; Colorado, R., Jr.; Wysocki, V. H.; Lee, T. R.; Lee, P. A.; Armstrong, N. R. Interface Dipoles Arising from Self-Assembled Monolayers on Gold: UV-Photoemission Studies of Alkanethiols and Partially Fluorinated Alkanethiols. *J. Phys. Chem. B* **2003**, *107*, 11690−11699.
(26) Hegner, M.; Wagner, P.; Semenza, G. Ultralarge Flat Template-Stripped Au Surfaces for Scanning Probe Microscopy. *Surf. Sci.* **1993**, *291*, 39−46.
(27) Wagner, P.; Hegner, M.; Guentherodt, H.; Semenza, G. Formation and in situ Modification of Monolayers Chemisorbed on Ultraflat Template-Stripped Gold Surfaces. *Langmuir* **1995**, *11*, 3867−3875.
(28) Borukhin, S.; Pokroy, B. Formation and Elimination of Surface Nanodefects on Ultraflat Metal Surfaces Produced by Template Stripping. *Langmuir* **2011**, *27*, 13415−13419.
(29) Heimel, G.; Romaner, L.; Zojer, E.; Brédas, J.-L. The Interface Energetics of Self-Assembled Monolayers on Metals. *Acc. Chem. Res.* **2008**, *41*, 721−729.
(30) Wimbush, K. S.; Fratila, R. M.; Wang, D.; Qi, D.; Liang, C.; Yuan, L.; Yakovlev, N.; Loh, K. P.; Reinhoudt, D. N.; Velders, A. H.; Nijhuis, C. A. Bias-Induced Transition from an Ohmic to a Nonohmic Interface in Supramolecular Tunneling Junctions with Ga_2O_3/EGaIn Top Electrodes. *Nanoscale* **2014**, *6*, 11246−11258.
(31) Johnson, M. S.; Kota, R.; Mattern, D. L.; Hill, C. M.; Vasiliu, M.; Dixon, D. A.; Metzger, R. M. A Two-Faced "Janus" Unimolecular Rectifier Exhibits Rectification Reversal. *J. Mater. Chem. C* **2014**, *2*, 9892−9902.
(32) Johnson, M. S.; Kota, R.; Mattern, D. L.; Metzger, R. M. Janus Reversal and Coulomb Blockade in Ferrocene-Perylenebisimide and N,N,N′,N′-Tetramethyl-para-phenylene-diamine-Perylenebisimide D-σ-A Rectifiers. *Langmuir* **2016**, *32*, 6851−6859.
(33) Chen, B.; Metzger, R. M. Rectification between 370 K and 105 K in Hexadecylquinolinium Tricyanoquinodimethanide. *J. Phys. Chem. B* **1999**, *103*, 4447−4451.
(34) Wan, A.; Jiang, L.; Suchand Sangeeth, C. S.; Nijhuis, C. A. Reversible Soft Top-Contacts to Yield Molecular Junctions with Precise and Reproducible Electrical Characteristics. *Adv. Funct. Mater.* **2014**, *24*, 4442−4456.
(35) Kim, H.; Segal, D. Controlling Charge Transport Mechanisms in Molecular Junctions: Distilling Thermally Induced Hopping from Coherent-Resonant Conduction. *J. Chem. Phys.* **2017**, *146*, No. 164702.
(36) Alami, F. A.; Soni, S.; Borrini, A.; Nijhuis, C. A. Perspective-Temperature Dependencies and Charge Transport Mechanisms in Molecular Tunneling Junctions Induced by Redox-Reactions. *ECS J. Solid State Sci. Technol.* **2022**, *11*, No. 055005.
(37) Vilan, A.; Aswal, D.; Cahen, D. Large-Area, Ensemble Molecular Electronics: Motivation and Challenges. *Chem. Rev.* **2017**, *117*, 4248−4286.
(38) Hines, T.; Diez-Perez, I.; Hihath, J.; Liu, H.; Wang, Z.-S.; Zhao, J.; Zhou, G.; Müllen, K.; Tao, N. Transition from Tunneling to Hopping in Single Molecular Junctions by Measuring Length and Temperature Dependence. *J. Am. Chem. Soc.* **2010**, *132*, 11658−11664.
(39) Ho Choi, S.; Kim, B.; Frisbie, C. D. Electrical Resistance of Long Conjugated Molecular Wires. *Science* **2008**, *320*, 1482−1486.

https://doi.org/10.1021/acsomega.2c01182
ACS Omega 2022, 7, 28790−28796